Nanoscale Patterning by UV Nanoimprint Lithography Using an Organometallic Resist

Canet Acikgoz,[†,‡] Boris Vratzov,[§] Mark A. Hempenius,[‡] G. Julius Vancso,[*,‡] and Jurriaan Huskens[*,†]

Molecular Nanofabrication Group and Materials Science and Technology of Polymers, MESA+ Institute for Nanotechnology, University of Twente, P.O. Box 217, 7500 AE Enschede, The Netherlands, and NT&D - Nanotechnology and Devices, 52062 Aachen, Germany

ARTICLE

ABSTRACT This paper presents the fabrication of poly(ferrocenylmethylphenylsilane) (PFMPS) patterns by step-and-flash imprint lithography for use as high-contrast etch masks in dry etch processes. PFMPS was spin-coated onto a resist template made by UV nanoimprint lithography to create a reactive ion etch resist layer with a thickness variation corresponding to the imprinted pattern. Etching back the excess of PFMPS by argon sputtering revealed the imprinted organic resist material, which was subsequently removed by oxygen plasma. PFMPS lines down to 30 nm were obtained after removal of the organic resist by oxygen plasma. Because PFMPS contains iron and silicon atoms in its main chain, it possesses a high resistance to oxygen reactive ion etching and, e.g., CHF_3/O_2 or SF_6/O_2 reactive ion etch processes. PFMPS patterns formed after imprinting were subsequently transferred into the underlying silicon substrate, and etch rates of 300 nm/min into Si and around 1 nm/min into the PFMPS layer were achieved, resulting in an etch contrast of approximately 300.

KEYWORDS: UV (light-assisted) nanoimprint lithography • poly(ferrocenylsilane)s • polymer resist • pattern transfer • reactive ion etching.

INTRODUCTION

Nanoimprint lithography (NIL) is an emerging nanopatterning technology that allows the fabrication of nanostructures with high resolution and complements an alternative to traditional photolithography. Among the imprint-based lithographic technologies, thermal NIL (1, 2) and UV-light-assisted NIL (UV-NIL) (3, 4) are the two techniques capable of replicating sub-10-nm features in a low-cost and high-throughput manner. The basic principle of these imprint-based techniques is that a rigid template or mold with prefabricated topographic features is used to replicate patterns within a resist layer, which can be subsequently employed as an etch mask for further pattern transfer. In thermal NIL, mold patterns are replicated into a thermoplastic material by heating the polymer above its glass transition temperature and applying pressure on the mold. The necessary but time-consuming temperature cycling gives rise to differences in the thermal expansion of resist, substrate, and template, leading to decreased throughput and improper overlay of the device layers and features (5). UV-NIL differs from thermal NIL because it is performed at room temperature and low pressure using low-viscosity, photocurable resists and a transparent, rigid template (6). This method does not require temperature cycling, leading to higher throughput than that in thermal NIL, and the transparency of the template offers the possibility for easy optical and high-precision alignment. UV-NIL uses a low-viscosity resist, which also beneficially influences the imprint force and compression time.

The major components of UV imprint resist materials are an organic acrylate, a cross-linker, and a photoinitiator. The resist may function as an etch mask for pattern transfer into the underlying substrate material (7). The availability of an appropriate UV-curing resist material is an important issue because the material has to fulfill several requirements such as low viscosity, low adhesion to the mold, good adhesion to the substrate, fast curing times, and high etch resistance to allow pattern transfer into the substrate (8). There are some commercially available UV-curable imprinting materials, but their characteristics and properties are still under study (9). The development of new resist materials for UV-NIL, therefore, remains crucial for enhancing the performance and scope of the technique.

Poly(ferrocenylsilane)s (PFSs) (10−12), containing iron and silicon atoms in the main chain, show very diverse and interesting properties. PFSs can be prepared by thermal ring-opening polymerization (ROP) of the corresponding silicon-bridged ferrocenophanes (13), by transition-metal-catalyzed ROP (14), and also by anionic polymerization (15). Especially the latter technique allows one to produce PFS homopolymers with controlled molar mass and low polydispersities. In addition, because of the living character of this polymerization, well-defined PFS containing block copolymers can be obtained with regular anionically polymerizable blocks such as polystyrene, polyisoprene, and many others (16, 17).

* Corresponding authors. E-mail: g.j.vancso@utwente.nl (G.J.V.), J.Huskens@utwente.nl (J.H.).
Received for review August 12, 2009 and accepted October 12, 2009
[†] Molecular Nanofabrication Group, MESA+ Institute for Nanotechnology, University of Twente.
[‡] Materials Science and Technology of Polymers, MESA+ Institute for Nanotechnology, University of Twente.
[§] NT&D - Nanotechnology and Devices.
DOI: 10.1021/am9005379
© 2009 American Chemical Society

Scheme 1. Fabrication Process for Creating PFMPS RIE Resist Patterns and Subsequent Pattern Transfer into the Underlying Substrate

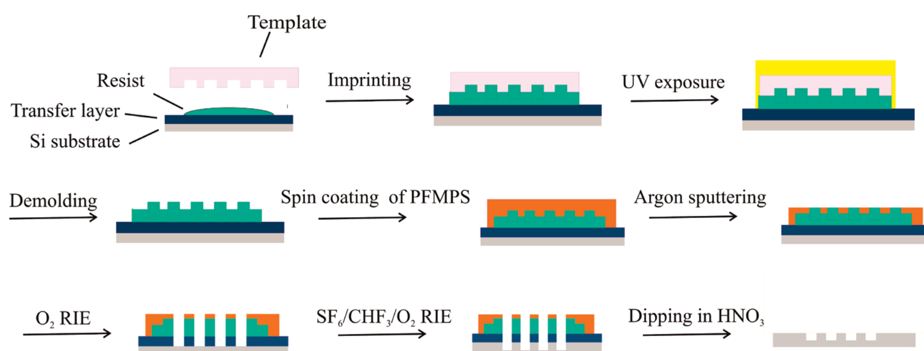

Because of the presence of iron and silicon atoms in the main chain, PFSs show a very high resistance to reactive ion etching (RIE) (18, 19). Oxygen plasma treatments lead to the formation of iron–silicon oxide layer domains in PFS-covered areas, which prevents further removal of PFS in oxygen RIE, while the high resistance to fluorocarbon and SF_6 RIE allows pattern transfer into silicon, silicon oxide, and silicon nitride substrates (18–20).

Methods for PFS-based lithography where generated patterns were transferred into various substrates include soft lithography, involving the use of PFS homopolymers as inks (21, 22), and block copolymer lithography where self-assembly of hybrid organic–organometallic block copolymers followed by etching led to nanoperiodic structures with feature sizes down to 20 nm in silicon substrates (20) and even in thin metal films (23). The use of poly(ferrocenylmethylphenylsilane) (PFMPS) as a thermal NIL resist was recently demonstrated by us (24). Polymer patterns formed after thermal imprinting were directly transferred into silicon substrates. In order to obtain high aspect ratios, the residual layer was completely removed by argon sputtering because direct etching without removal of the residual layer gave rise to oxide layer formation, which prevented further pattern transfer. Although the direct thermal imprinting process into PFMPS enabled us to transfer the patterns into the substrate, shortcomings were observed when the feature sizes became smaller. Small features below 100 nm were not transferred faithfully into the substrate because they were damaged during argon sputtering. Additional benefits of UV-NIL such as higher throughput and elimination of thermal cycling, as discussed above, make the development of a UV-NIL process based on PFSs desirable.

Here, patterns of PFMPS were created on a template made by step-and-flash imprint lithography (S-FIL) using a UV-curable resist (25). This approach is an example of a bilayer-type S-FIL process because two different materials are used with different etch selectivities (26) and PFMPS is used as the top resist. The choice of the top resist is critical for successful dry etching into silicon substrates because the masking layer that is to be etched should have a distinctly different etch selectivity over the underlying UV-curable resist. After patterning of the UV-curable resist, PFMPS is spin-coated onto the imprinted structures to form bilayer structures and subsequent treatment with argon and oxygen plasma provides patterns of PFMPS with good reproducibility because of the high etch contrast between the two polymers. The process prevents the formation of a residual layer of PFMPS and thus its cumbersome removal (24), which thus constitutes an advantage over the direct hot embossing of PFMPS. The technique allows the possibility of creating etch-resistant patterns of PFMPS with sizes down to the nanometer range. Moreover, using PFMPS in this process allows control of the critical dimensions. Because it is a bilayer process, the final pattern size is not defined by imprinting alone but also by subsequent etch processes, which makes the role of PFMPS highly important. It provides a very high selectivity over UV-curable resist because of its high iron and silicon content, which is difficult to obtain with other imprint materials.

RESULTS AND DISCUSSION

PFMPS was chosen as a resist, because it is an amorphous polymer due to the unsymmetric substitution on the silicon atom in the main chain. The use of an amorphous polymer is essential since crystallization may destroy the imprinted patterns. Also, PFMPS forms homogeneous films. Scheme 1 summarizes the bilayer-type S-FIL process which consists of the fabrication of patterns of a UV-curable monomer, deposition of PFMPS on this template, and the etch sequence steps for transferring the patterns into the substrate. The imprint material was dispensed onto the transfer layer-coated substrates and the template was brought into contact with the still liquid imprint material. The transfer layer provided a good adhesion of the imprint material to the substrate. After exposure and curing of the imprint material, the template was demolded from the substrate, leaving its negative 3D image. The PFMPS was spin coated on top of the imprinted structures, creating an organometallic layer with a corresponding thickness variation. Argon plasma treatment was performed to homogeneously etch down the polymer in order to expose the organic imprint material. Subsequent treatment with oxygen plasma led to removal of the exposed organic imprint material and the PFMPS lines were transferred into the substrate, leading to pattern inversion.

The S-FIL^{TM} method (25) used to create patterns on a substrate, consisting of lines of 100 nm wide with pitches of 1:1, 1:2 and 1:3 and with a height of 100 nm, is shown in

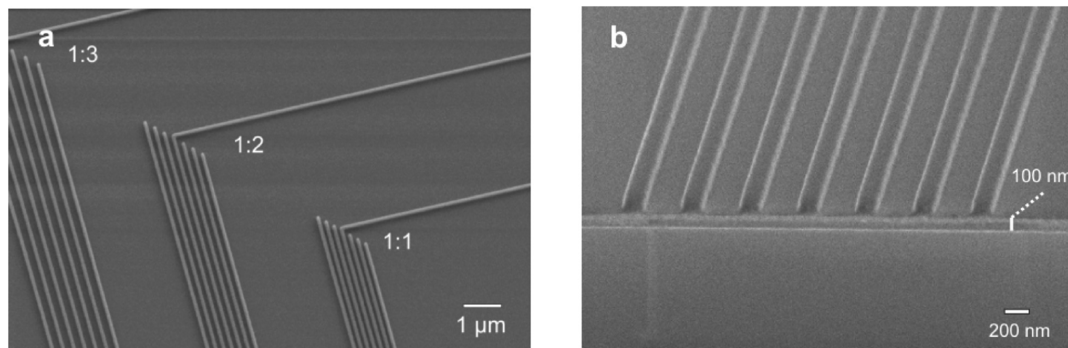

FIGURE 1. SEM images of UV-imprinted structures of (a) lines of 100 nm wide with pitches of 1:1, 1:2 and 1:3 and with a height of 100 nm (b) lines of 100 nm height showing the total thickness of the residual UV-curable resist layer and the transfer layer.

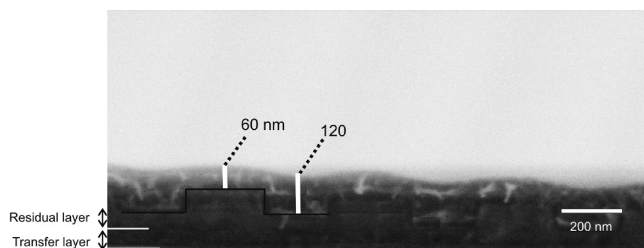

FIGURE 2. SEM image of a PFMPS layer spin coated on top of imprinted resist lines.

Figure 1. Figure 2 shows a cross-section image of the imprinted lines after spin-coating PFMPS onto the imprinted structures. As seen in the cross section SEM image in Figure 2, the thickness of the transfer layer was 60 nm and the residual UV-curable resist layer after imprinting was about 40−50 nm. The dispensing conditions were optimized to obtain such thin residual layers after imprinting. Since the dispensed monomer was cross-linked upon UV curing, spin coating of a solution of PFMPS in toluene did not affect the resist patterns. The thickness of the PFMPS polymer between the resist lines after spin-coating was determined to be 120 nm, while on top of the UV-imprinted structures it was about 60 nm. It is crucial to adjust the layer thickness to planarize the features. The PFMPS thickness applied here appeared to be sufficient for covering the nanometer and micrometer features completely with sufficient planarization (see also Figure 3, below). The PFMPS provided good wetting and adhesion performance to the imprint material which is important for subsequent processing.

The PFMPS layer was etched back homogeneously in an argon plasma to reveal the top of the imprinted structures (Figure 3). The etch rate of PFMPS upon argon sputtering was determined to be 1.5 nm min^{-1}. Taking this etch rate into consideration, the time of the argon sputtering treatment was varied from 15 to 25 min. A time of 15 min proved to be insufficient for exposing the resist lines (Figure 3a), whereas after 25 min the PFMPS layer was removed, while the resist line shapes were not affected adversely (Figure 3b, c). Opening of the imprinted areas could only be achieved by argon sputtering since oxygen plasma results in highly etch resistant oxide formation, as mentioned before (24).

The argon sputtering step was followed by O_2 RIE during which the exposed organic imprint layer and the transfer layer material underneath were selectively etched through. During this treatment, the PFMPS was oxidized to form a hard Fe/Si oxide layer which allowed further pattern transfer into the substrate (18). The O_2 RIE etch rates of PFMPS and the organic imprint material were found to be 1 and 60 nm/min, respectively, which results in an etch selectivity of 60. Two minutes of treatment with oxygen plasma was sufficient to remove the imprint material down to the substrate as shown in Figures 4a and 4b for features of 80 and 30 nm lines, respectively. PFMPS lines down to 30 nm were obtained after oxygen plasma treatment as shown in Figure 4b. The PFMPS lines revealed a line width roughness of about 5 nm (for the thinner lines, Figure 4b), which is similar to the edge roughness of the lines on the template used during imprinting. The imprint and sputtering processes apparently did not add additional line width roughness to the PFMPS features.

Figure 4a and 4b show the occurrence of some degree of undercutting upon extension of the O_2 plasma treatment. Figure 4c demonstrates the undercut profile obtained upon increasing the oxygen plasma treatment to 2.5 min. Nevertheless, the material in between the PFMPS lines was completely removed while the width of the PFMPS areas remained intact, which are required for transferring these lines into the underlying substrate.

Upon pattern transfer into the underlying Si substrate, RIE with CHF_3 and SF_6 was tested. The thickness of the PFMPS etch mask remained almost the same upon exposure to CHF_3 and SF_6 plasmas. Etch rates of 300 nm/min into Si and around 1 nm/min into the PFMPS layer were found, resulting in an etch contrast of approximately 300. Different etch profiles were obtained by tuning the composition of the gas mixture in the plasma. Figure 5a shows the lines etched with a mixture of CHF_3 (25 sccm), O_2 (20 sccm) and SF_6 (30 sccm) for 1 min (27). Figure 5b shows the etching profile attained after decreasing the amount of CHF_3 and SF_6 in the plasma while keeping the amount of oxygen constant. The profile has a rounded shape for the mixture of CHF_3 (20 sccm) and SF_6 (24 sccm). A decrease in CHF_3 (18 sccm) and SF_6 (20 sccm) resulted in profiles which were tapered with an aspect ratio of 3 in case of 2 min of etching (Figure 5c). The profile became more vertical with a flat surface at the bottom after a 10% decrease in the amount of CHF_3 and SF_6 (Figure 5d).

The different profiles obtained can be correlated to the oxygen content in the plasma. Increase in the relative

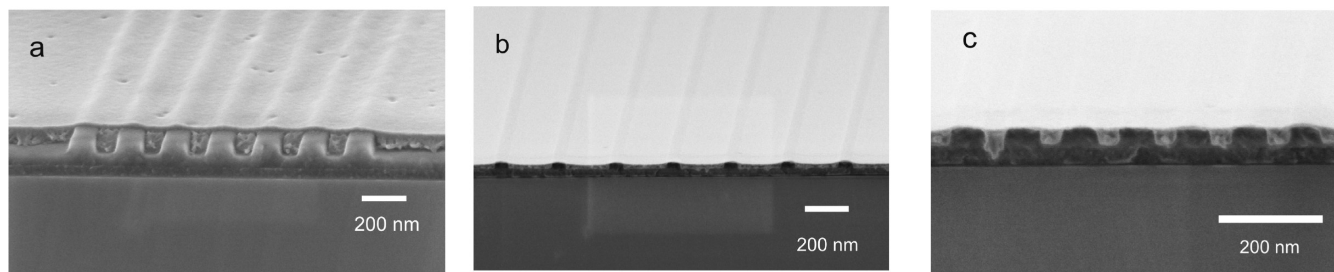

FIGURE 3. SEM images of PFMPS structures after argon plasma treatment to expose the imprinted lines (a) for 15 min, and (b, c) for 25 min. Prior to argon sputtering, PFMPS was spin coated on top of the UV-imprinted resist lines.

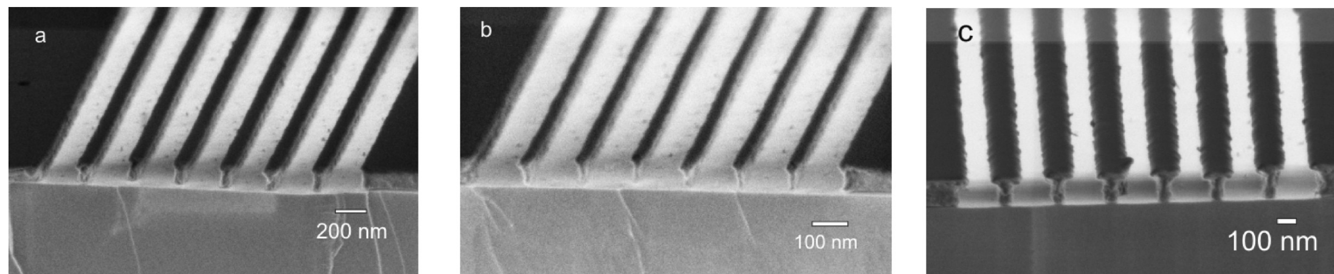

FIGURE 4. SEM images of lines fabricated after O_2 RIE of (a) 80 nm PFMPS lines and (b) 30 nm PFMPS lines after 2 min of treatment. (c) 100 nm PFMPS lines after a 2.5 min treatment. Prior to O_2 RIE, the samples were coated with PFMPS and then etched back for 25 min by argon sputtering. The dark stripes in the images correspond to PFMPS lines.

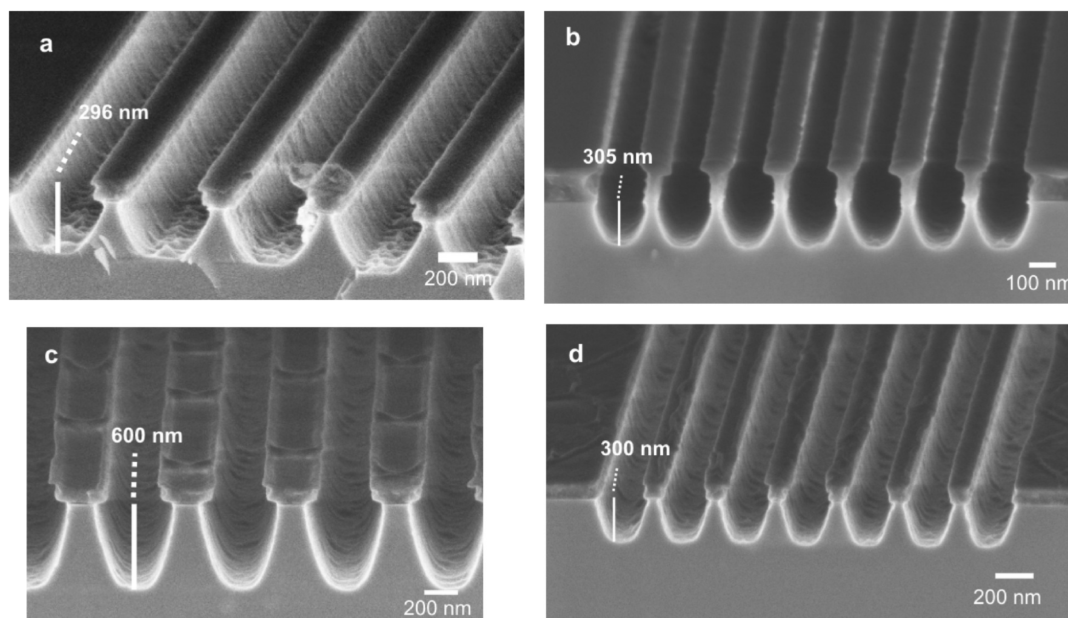

FIGURE 5. SEM images of samples etched with $CHF_3/O_2/SF_6$ (gas flow rates in sccm) (a) (25/20/30) for 1 min for 200 nm lines (b) 20/20/ 24 for 1 min for 100 nm lines (c) 18/20/20 for 2 min for 200 nm lines (d) 16/ 20/18 for 1 min for 100 nm lines. Organometallic resist material is still present on top of the lines.

oxygen content likely enhances passivation of the vertical silicon surfaces with an SiO_xF_y layer and therefore enables the process to become more anisotropic (28). It was also observed that changes in pattern dimensions can influence the etching characteristics. In Figure 6a, the walls obtained were more vertical than the line patterns in Figure 6b, even though they were treated under the same plasma conditions.

Figure 6 exemplifies the stability of the PFMPS resist after exposure to an O_2 containing plasma. Even though the resist is very stable, it could be easily removed in dilute nitric acid followed by sonication in toluene. Figure 7a demonstrates grooves fabricated in Si with an aspect ratio of 3 after 3 min of wet etching and Figure 7b shows 500 nm lines with an aspect ratio of 1 after 1 min of etching followed by removal of the resist material.

CONCLUSIONS

We have shown the fabrication of polymeric structures with lateral dimensions down to 30 nm and aspect ratios of up to 3 in a bilayer-type UV-NIL process. The organometallic polymer PFMPS was spin-coated onto a UV-NIL patterned substrate, followed by an argon plasma treatment to expose the imprint material. Removal of the imprint material with oxygen plasma gave rise to PFMPS patterns forming a

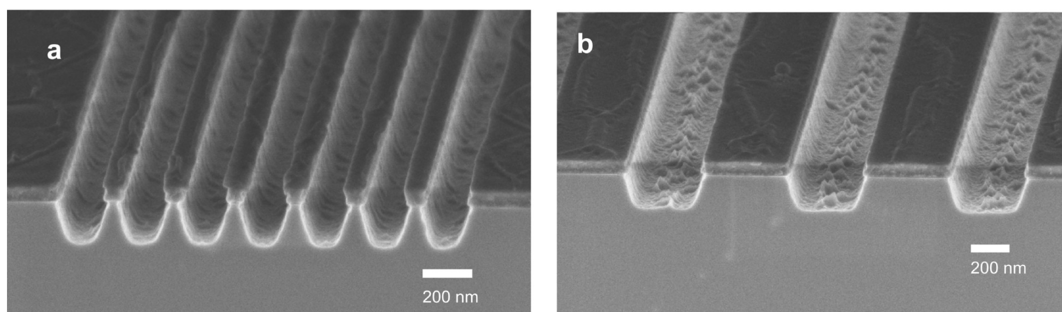

FIGURE 6. Profile obtained after treatment with $CHF_3/O_2/SF_6$ (in sccm) 16/20/18 during 1 min (a) for 100 nm lines (b) for 500 nm lines.

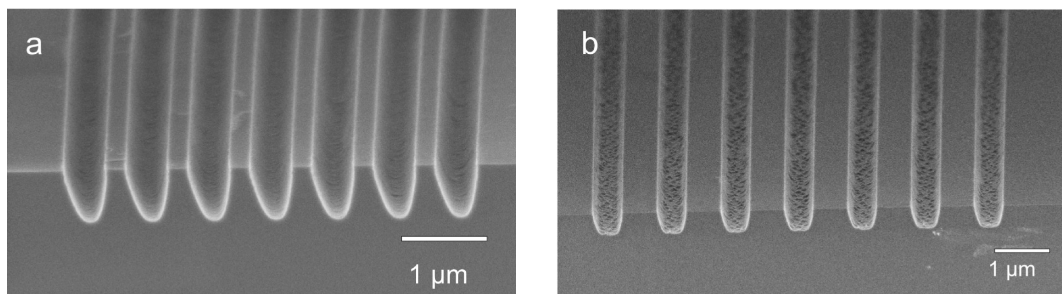

FIGURE 7. SEM images of fabricated lines after removal of resist material, imprint material and transfer layer in dilute nitric acid and toluene (a) after etching with a mixture of CHF_3 (18 sccm), O_2 (20 sccm) and SF_6 (20 sccm) for 500 nm lines for 2 min and (b) after etching with a mixture of CHF_3 (16 sccm), O_2 (20 sccm) and SF_6 (18 sccm) for 1 μm lines for 1 min.

negative replica of the template employed. Pattern transfer into silicon sustrates was accomplished by the use of a $CHF_3/SF_6/O_2$ plasma. Variations of the plasma composition led to different etch profiles. This process offers the possibility for combining the advantages of UV-NIL with the high etch resistance of PFSs to produce features sizes down to the sub-100 nm range, and may be of use in areas such as data storage, microelectronics and bioelectronics.

EXPERIMENTAL SECTION

Polymer Synthesis. [1]Methylphenylsilaferrocenophane was prepared as described earlier (16, 29). The monomer was purified by several crystallizations from *n*-heptane at −70 °C followed by vacuum sublimation. Transition-metal-catalyzed ROP of [1]methylphenylsilaferrocenophane was carried out in the presence of Et_3SiH with the addition of Karstedt's catalyst (14). The polymer was then precipitated in *n*-heptane. Molar mass characteristics of the polymer were determined by gel permeation chromatography measurements in tetrahydrofuran using polystyrene calibration. $M_w = 49\ 501$ g/mol, $M_n = 44\ 643$ g/mol, and $M_w/M_n = 1.109$.

Pattern Fabrication. Patterns were generated using UV-based nanoimprint technology. All of the imprints were carried out on an Imprio 55 from Molecular Imprints Inc., using their S-FIL process (25). As a substrate, double-sided, polished Si wafers were used, which were also coated with a thin transfer layer applied by spin coating and hot baking in order to achieve good adhesion of the imprint material to the substrate. DUV 30J was used as the transfer layer. The quartz template employed for the imprints consisted of lines with feature sizes from tens of microns to below 50 nm. Prior to imprinting, the template was treated with a release layer in order to prevent sticking of the imprint material to the template. The release layer used was perfluoro-1,1,2,2-tetrahydrooctyltrichlorosilane, which is used to modify the template surface energy. The surface treatment procedure used in this process started with the cleaning of the template with a piranha solution (concentrated H_2SO_4 and 33% aqueous H_2O_2 in a 3:1 volume ratio; **Warning!** *piranha should be handled with caution; it can detonate unexpectedly!*) for 30 min to remove any surface organic contaminants. After the piranha treatment, the substrates were blown dry with N_2 and reacted with alkyltrichlorosilane (6). Imprinting was performed using a low-viscosity acrylate-based organic S-FIL resist (Monomat, Molecular Imprints Inc.). The imprint material was deposited by direct dispensing, where the volume was locally adjusted to the pattern definition. After dispensing, the template was pressed into the still liquid imprint material and held for 20 s under a pressure of 50 mbar to fill all of the features. Thereafter, the imprint material was cured by UV-light irradiation through the transparent template, followed by demolding.

Pattern Transfer. The synthesized PFMPS was spin-coated on top of the imprinted resist. Argon plasma sputtering was applied for 20−25 min (Ion Beam Etcher, 350 V, 6 mA) in order to expose the organic imprint material. The imprinted resist features were subsequently etched with oxygen plasma to expose the PFMPS lines. Oxygen reactive ion etching to remove the imprinted resist was performed in an Elektrotech PF 340 apparatus (8 mTorr, 50 W, 20 sccm O_2). Etching into the substrate using the PFMPS lines as a template was enabled with different mixtures of CHF_3, O_2, and SF_6 at a pressure of 10 mTorr. The resist was stripped off by sonication for 1 h in a 10% nitric acid solution followed by sonication in toluene.

SEM characterization was performed with a HR-LEO 1550 FEF scanning electron microscope.

Acknowledgment. The MESA$^+$ Institute for Nanotechnology (SRO Nanofabrication) is acknowledged for financial support. We thank Mark Smithers for acquiring the SEM images.

REFERENCES AND NOTES

(1) Chou, S. Y.; Krauss, P. R.; Renstrom, P. J. *Appl. Phys. Lett.* **1995**, *67*, 3114–3116.
(2) Chou, S. Y.; Krauss, P. R.; Renstrom, P. J. *Science* **1996**, *272*, 85–87.
(3) Bender, M.; Otto, M.; Hadam, B.; Vratzov, B.; Spangenberg, B.; Kurz, H. *Microelectron. Eng.* **2000**, *53*, 233–236.

(4) Colburn, M.; Johnson, S.; Stewart, M.; Dample, S.; Bailey, T.; Choi, B.; Wedlake, M.; Michaelson, T.; Sreenivasan, S. V.; Ekerdt, J. G.; Willson, C. G. *Proc. SPIE* **1999**, *37*, 9–389.
(5) Stewart, M. D.; Johnson, S. C.; Sreenivasan, S. V.; Resnick, D. J.; Willson, C. G. *J. Microlithogr. Microfabr. Microsyst.* **2005**, *4*, 1537–1546.
(6) Bailey, T.; Choi, B. J.; Colburn, M.; Meissl, M.; Shaya, S.; Ekerdt, J. G.; Sreenivasan, S. V.; Willson, C. G. *J. Vac. Sci. Technol. B* **2000**, *18*, 3572–3577.
(7) Choi, J. H.; Lee, S. W.; Choi, D. G.; Kim, K. D.; Jeong, J. H.; Lee, E. S. *J. Vac. Sci. Technol. B* **2008**, *26*, 1390–1394.
(8) Schmitt, H.; Frey, L.; Ryssel, H.; Rommel, M.; Lehrer, C. *J. Vac. Sci. Technol. B* **2007**, *25*, 785–790.
(9) Sakai, N.; Taniguchi, J.; Kawaguchi, K.; Ohtaguchi, M.; Hirasawa, T. *J. Photopolym. Sci. Technol.* **2005**, *18*, 531–536.
(10) Eloi, J. C.; Chabanne, L.; Whittell, G. R.; Manners, I. *Mater. Today* **2008**, *11*, 28–36.
(11) Kulbaba, K.; Manners, I. *Macromol. Rapid Commun.* **2001**, *22*, 711–724.
(12) Whittell, G. R.; Manners, I. *Adv. Mater.* **2007**, *19*, 3439–3468.
(13) Foucher, D. A.; Tang, B. Z.; Manners, I. *J. Am. Chem. Soc.* **1992**, *114*, 6246–6248.
(14) Gomez Elipe, P.; Macdonald, P. M.; Manners, I. *Angew. Chem., Int. Ed. Engl.* **1997**, *36*, 762–764.
(15) Rulkens, R.; Ni, Y. Z.; Manners, I. *J. Am. Chem. Soc.* **1994**, *116*, 12121–12122.
(16) Ni, Y. Z.; Rulkens, R.; Manners, I. *J. Am. Chem. Soc.* **1996**, *118*, 4102–4114.
(17) Kloninger, C.; Rehahn, M. *Macromolecules* **2004**, *37*, 1720–1727.
(18) Lammertink, R. G. H.; Hempenius, M. A.; Chan, V. Z. H.; Thomas, E. L.; Vancso, G. J. *Chem. Mater.* **2001**, *13*, 429–434.
(19) Korczagin, I.; Lammertink, R. G. H.; Hempenius, M. A.; Golze, S.; Vancso, G. J. *Ordered Polymeric Nanostructures at Surfaces*; Springer: Berlin, 2006; Vol. 200, pp 91−117.
(20) Lammertink, R. G. H.; Hempenius, M. A.; van den Enk, J. E.; Chan, V. Z. H.; Thomas, E. L.; Vancso, G. J. *Adv. Mater.* **2000**, *12*, 98–103.
(21) Korczagin, I.; Golze, S.; Hempenius, M. A.; Vancso, G. J. *Chem. Mater.* **2003**, *15*, 3663–3668.
(22) Hempenius, M. A.; Lammertink, R. G. H.; Peter, M.; Vancso, G. J. *Macromol. Symp.* **2003**, *196*, 45–56.
(23) Cheng, J. Y.; Ross, C. A.; Chan, V. Z. H.; Thomas, E. L.; Lammertink, R. G. H.; Vancso, G. J. *Adv. Mater.* **2001**, *13*, 1174–1178.
(24) Acikgoz, C.; Hempenius, M. A.; Vancso, G. J.; Huskens, J. *Nanotechnology* **2009**, *20*, 135304.
(25) Resnick, D.; Sreenivasan, S. V.; Willson, C. G. *Mater. Today* **2005**, 34.
(26) Sreenivasan, S. V.; McMackin, I.; Xu, F.; Wang, D.; Stacey, N. *Micro Magazine* **2005**.
(27) Jansen, H.; Deboer, M.; Legtenberg, R.; Elwenspoek, M. *J. Micromech. Microeng.* **1995**, *5*, 115–120.
(28) Legtenberg, R.; Jansen, H.; Deboer, M.; Elwenspoek, M. *J. Electrochem. Soc.* **1995**, *142*, 2020–2028.
(29) Temple, K.; Massey, J. A.; Chen, Z. H.; Vaidya, N.; Berenbaum, A.; Foster, M. D.; Manners, I. *J. Inorg. Organomet. Polym.* **1999**, *9*, 189–198.

AM9005379